

Wave-induced oscillations in harbours of arbitrary geometry

By JIIN-JEN LEE

W. M. Keck Laboratory of Hydraulics and Water Resources,
California Institute of Technology

(Received 20 March 1970)

Wave-induced oscillations in harbours of constant depth but arbitrary shape in the horizontal plane connected to the open-sea are investigated both theoretically and experimentally. A theory termed the 'arbitrary-shape harbour' theory is developed. The solution of the Helmholtz equation is formulated as an integral equation which is then approximated by a matrix equation. The final solution is obtained by equating, at the harbour entrance, the wave amplitudes and their normal derivatives obtained from the solutions for the regions outside and inside the harbour. Special solutions using the method of separation of variables for the region inside circular and rectangular harbours are also obtained. Experiments were conducted to verify the theories. Four specific harbours were investigated: two circular harbours with 10° and 60° openings respectively, a rectangular harbour, and a model of the East and West Basins of Long Beach Harbour, California. In each case, the theoretical results agreed well with the experimental data.

1. Introduction

A natural or an artificial harbour can exhibit frequency- (or period-) dependent water surface oscillations when excited by incident waves in a way which is similar to the dynamic response of mechanical or acoustical systems when exposed to time-varying forces, pressures, or displacements. Such oscillations in harbours can cause significant damage to moored ships and adjacent structures as well as inducing undesirable currents in harbours.

Many previous investigators have studied various aspects of the harbour resonance problem. McNown (1952) investigated the response characteristics of a circular harbour of small entrance gap by assuming that the crest of a standing wave (antinode) occurred at the entrance when the harbour was in resonance. A similar method was applied to rectangular harbours by Kravtchenko & McNown (1955). Thus, for resonant motions such a hypothesis led to a boundary condition identical to that for a completely closed basin. Therefore the wave periods associated with resonant oscillations would be those which correspond to the eigenvalues for the free oscillations of a circular (or a rectangular) basin. This imposed condition at the harbour entrance is unsatisfactory in the sense that the slope of the water surface at the entrance should be part of the solution of the problem and should not be imposed in advance.

The problem of a rectangular harbour connected directly to the open-sea has been investigated by Miles & Munk (1961). This important contribution included the effect of the wave radiation from the harbour mouth to the open-sea thereby limiting the maximum wave amplitude within the harbour for the inviscid case to a finite value even at resonance. They considered an arbitrary-shape harbour and formulated the problem as an integral equation in terms of a Green's function. Unfortunately, as they have noted, the Green's function for an arbitrary-shape harbour is very difficult to determine. Thus, this general formulation was applied to a specialized shape: a rectangular harbour, and it was found that a narrowing of the harbour entrance leads not to a reduction in harbour surging (oscillation), but to an enhancement. This result was termed by them the 'harbour paradox'.

Ippen & Goda (1963) also studied the problem of a rectangular harbour connected to the open-sea. In that analysis, the waves radiated from the harbour entrance to the open-sea were evaluated using the Fourier transformation method while the solution inside the harbour was obtained by the method of separation of variables. The complete solution was obtained by matching the average wave amplitude at the harbour entrance obtained from solutions in both regions. Good agreement was found between the theory and experiments.

Wilson, Hendrickson & Kilmer (1965) studied long wave oscillations in a basin of variable depth open at one end using a finite-difference method where the boundary condition at the harbour entrance must be properly assumed. Leendertse (1967) has also developed a finite-difference numerical scheme for the propagation of long-period waves in an arbitrary-shaped basin given the water surface elevations at the open boundary. Recently, Hwang & Tuck (1970) developed a method to analyze the problem of wave-induced oscillations in a harbour of arbitrary shape and constant depth. Their method of approach is to superimpose scattered waves which are caused by the presence of the boundary on the standing wave system. The scattered waves are computed using a distribution of sources along the coastline and the boundary of the harbour with unknown strengths to be determined numerically. The calculation of the source strengths along the entire reflecting boundary must be terminated at some distance from the entrance. However, for an arbitrary-shape harbour the position at which the calculation of the source strength can be terminated is not obvious unless trial solutions are made.

The present work is to develop a theory for the wave-induced oscillations in harbours of arbitrary geometry (with constant depth) by applying Weber's solution of the Helmholtz equation in both the regions inside and outside the harbour with the final solution obtained by matching the wave amplitudes and their normal derivatives at the entrance. Theories for special-shaped harbours are also developed which can be used for analytical checks for the general theory. Experiments were performed in the laboratory basin in order to verify the theoretical solutions.

2. Theoretical analysis

Assuming an irrotational flow, one can define a velocity potential Φ such that the fluid particle velocity vector can be expressed as $\mathbf{u} = \nabla\Phi$. Thus, from the continuity equation for an incompressible fluid, Laplace's equation is obtained:

$$\nabla \cdot \mathbf{u} = \nabla^2\Phi = 0. \quad (1)$$

A solution of Φ is sought in the following form:

$$\Phi(x, y, z; t) = \frac{1}{-i\sigma} f(x, y) Z(z) \exp(-i\sigma t), \quad (2)$$

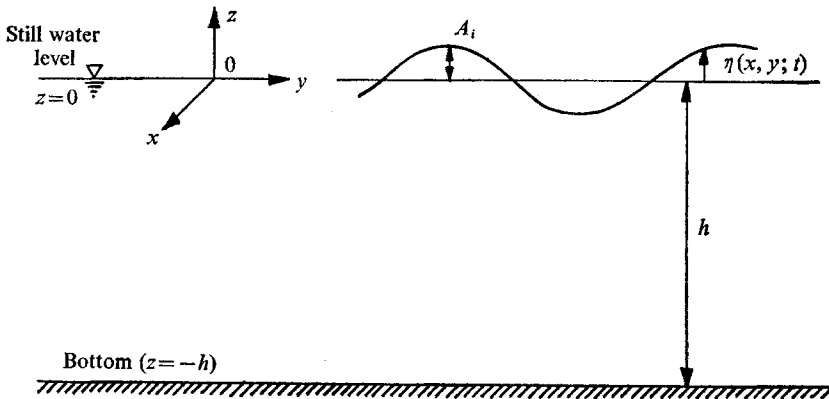


FIGURE 1. Definition sketch of the co-ordinate system.

where σ is the angular frequency defined as $2\pi/T$ (T is the wave period), $i = \sqrt{-1}$, and $f(x, y)$ is termed the wave function which describes the variation of Φ in x, y direction. (The co-ordinate system is defined in figure 1.) Substituting (2) into (1) one obtains

$$\frac{1}{f} \left(\frac{\partial^2 f}{\partial x^2} + \frac{\partial^2 f}{\partial y^2} \right) = -\frac{1}{Z} \frac{\partial^2 Z}{\partial z^2}. \quad (3)$$

If (3) is set to be equal to a constant, say $-k^2$, then the following set of equations is obtained:

$$\frac{d^2 Z}{dz^2} - k^2 Z = 0, \quad (4)$$

$$\frac{\partial^2 f}{\partial x^2} + \frac{\partial^2 f}{\partial y^2} + k^2 f = 0. \quad (5)$$

The boundary condition at the bottom and the linearized dynamic free-surface condition respectively are:

$$\partial\Phi(x, y, -h; t)/\partial z = 0, \quad (6a)$$

$$\eta(x, y; t) = A_i f(x, y) \exp(-i\sigma t) = -(1/g) (\partial\Phi/\partial t)_{z=0}, \quad (6b)$$

where the depth y is assumed constant, η is the displacement of water surface from the still water level, A_i is the amplitude at the crest of the incident wave, and g is the acceleration of gravity.

The function $Z(z)$ which satisfies (4) and (6) can be found as

$$Z(z) = -\frac{A_i g \cosh k(h+z)}{\cosh kh}.$$

Thus, the velocity potential Φ becomes:

$$\Phi(x, y; t) = \frac{1}{i\sigma} \frac{A_i g \cosh k(h+z)}{\cosh kh} f(x, y) \exp(-i\sigma t). \quad (7)$$

Substituting (6b) and (7) into the linearized kinematic free surface condition, $\partial\eta/\partial t = (\partial\Phi/\partial z)_{z=0}$, the well known 'dispersion relation' for water waves is obtained: $\sigma^2 = gk \tanh(kh)$; therefore, the arbitrary constant used in (4) and (5) is the wave-number k which appears in the dispersion relation and is defined as $2\pi/L$ (L is the wavelength).

In order to complete the expression for the velocity potential Φ , the main problem which remains is to determine the wave function $f(x, y)$ which satisfies (5) (commonly known as the Helmholtz equation) and the boundary condition that there is no flow through solid boundaries (such as the coastline and the boundary of the harbour) and also the radiation condition which will be discussed later.

In § 2.1 a method for solving the Helmholtz equation (5), for an arbitrary-shape harbour will be presented, thereby allowing one to determine the wave-induced oscillations in such a harbour.

2.1. Arbitrary-shape harbour theory

The main idea behind the development of the theory of the response of an arbitrary-shape harbour to incident waves is as follows:

(i) The domain of interest shown in figure 2 is divided at the harbour entrance into two regions: the infinite ocean region (region I), and the region bounded by the limits of the harbour (region II).

(ii) The function f_1 is determined in region I in terms of $\partial f_1/\partial n$ at the harbour entrance; likewise, the function f_2 is evaluated in region II in terms of $\partial f_2/\partial n$ at the entrance. (Both f_1 and f_2 satisfy (5).)

(iii) The 'continuity condition' at the harbour entrance, i.e.

$$f_1 = f_2 \quad \text{and} \quad \partial f_1/\partial n = -\partial f_2/\partial n,$$

is used to solve for the derivative $\partial f_2/\partial n$ (or $\partial f_1/\partial n$); thus, the function f_2 in region II (inside the harbour) can be evaluated.

(1) *Function f_2 inside the harbour (region II)*. By applying Green's identity formula in region II and choosing the Hankel function of the first kind and zeroth order, $H_0^{(1)}(kr)$, to be the fundamental solution of the two-dimensional Helmholtz equation, (5), the function f_2 at any position \mathbf{x} inside the harbour can be expressed as (this is referred to as Weber's solution of the Helmholtz equation, see Baker & Copson (1950), Banaugh & Goldsmith (1963), also Lee (1969))

$$f_2(\mathbf{x}) = -\frac{1}{4}i \int_s \left\{ f_2(\mathbf{x}_0) \frac{\partial}{\partial n} [H_0^{(1)}(kr)] - H_0^{(1)}(kr) \frac{\partial}{\partial n} f_2(\mathbf{x}_0) \right\} ds(\mathbf{x}_0), \quad (8)$$

where \mathbf{x}_0 is the position vector of the boundary point, r is the distance $|\mathbf{x} - \mathbf{x}_0|$, and n is directed outward and normal to the boundary. The integration indicated by (8) is to be performed along the boundary of the harbour travelling in a counter-clockwise direction.

The boundary condition set previously states that $\partial f_2 / \partial n$ is zero on the solid boundary of the harbour, but its value at the harbour entrance is unknown.

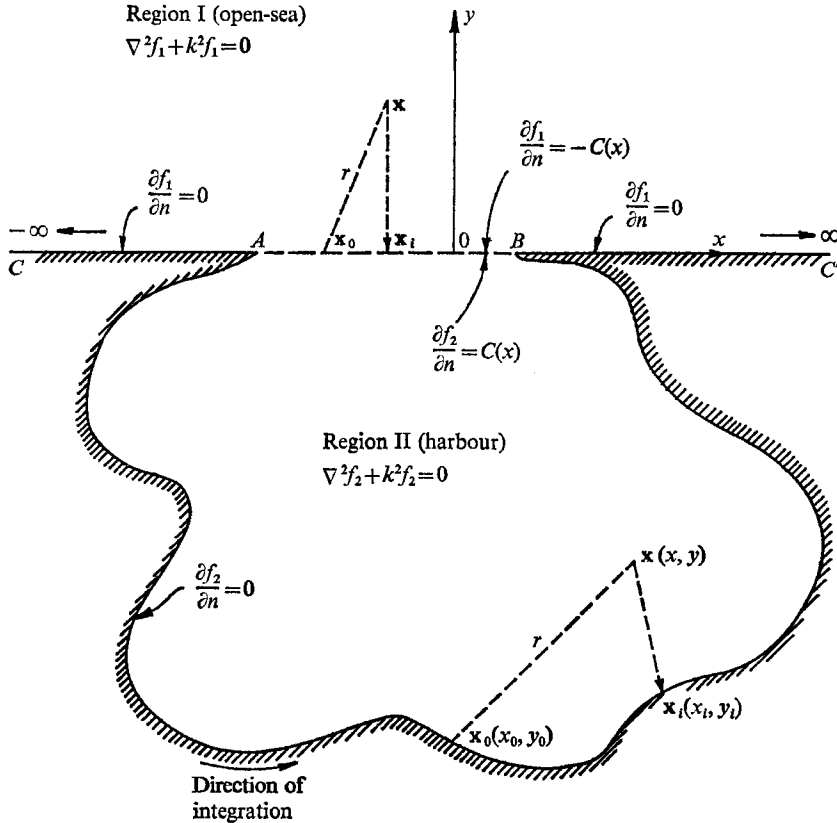


FIGURE 2. Definition sketch of an arbitrary-shape harbour.

The value of f_2 on the boundary at this stage of the development is still unknown. In order to determine the value of f_2 on the boundary as a function of $\partial f_2 / \partial n$ at the harbour entrance, (8) is modified by allowing the field point \mathbf{x} to approach a boundary point $\mathbf{x}_i(x_i, y_i)$ from the interior of the harbour (see figure 2). If the boundary is sectionally smooth the following expression can be obtained (see Lee (1969) for the derivation of this expression and also for the case of a boundary with sharp corners).

$$f_2(\mathbf{x}_i) = -\frac{1}{4}i \int_s \left\{ f_2(\mathbf{x}_0) \frac{\partial}{\partial n} [H_0^{(1)}(k|\mathbf{x}_i - \mathbf{x}_0|)] - H_0^{(1)}(k|\mathbf{x}_i - \mathbf{x}_0|) \frac{\partial}{\partial n} [f_2(\mathbf{x}_0)] \right\} ds(\mathbf{x}_0) + \frac{1}{2}f_2(\mathbf{x}_i). \quad (9)$$

Rearranging (9) one obtains the following integral equation for the function $f_2(\mathbf{x}_i)$ on the boundary of the harbour:

$$f_2(\mathbf{x}_i) = -\frac{1}{2}i \int_s \left\{ f_2(\mathbf{x}_0) \frac{\partial}{\partial n} [H_0^{(1)}(k|\mathbf{x}_i - \mathbf{x}_0|)] - H_0^{(1)}(k|\mathbf{x}_i - \mathbf{x}_0|) \frac{\partial}{\partial n} [f_2(\mathbf{x}_0)] \right\} ds(\mathbf{x}_0). \tag{10}$$

To solve (10) for the function $f_2(\mathbf{x}_i)$ an approximate method is proposed. The boundary of the harbour is divided into a sufficiently large number of segments (N) and the value of f_2 (or $\partial f_2/\partial n$) at each segment is considered constant and equal to the value at the mid-point of each segment. Thus, writing (10) in discrete form one obtains:

$$f_2(\mathbf{x}_i) = -\frac{1}{2}i \sum_{j \neq i}^N \left[f_2(\mathbf{x}_j) \frac{\partial}{\partial n} (H_0^{(1)}(kr_{ij})) - H_0^{(1)}(kr_{ij}) \frac{\partial}{\partial n} f_2(\mathbf{x}_j) \right] \Delta s_j - \frac{1}{2}i f_2(\mathbf{x}_i) \int_0^{\frac{1}{2}\Delta s_i} 2 \left(-kH_1^{(1)}(kr) \frac{\partial r}{\partial n} \right) dr + \frac{1}{2}i \frac{\partial f_2}{\partial n}(\mathbf{x}_i) \int_0^{\frac{1}{2}\Delta s_i} 2H_0^{(1)}(kr) dr. \tag{11}$$

Equation (11) can be rewritten as a matrix equation,

$$\mathbf{X} = -\frac{1}{2}i(G_n \mathbf{X} - \mathbf{GP}), \tag{12}$$

in which the following notation is used:

$$\mathbf{X} = f_2(\mathbf{x}_i), \quad (i = 1, 2, \dots, N); \tag{13a}$$

$$\mathbf{P} = \frac{\partial}{\partial n} f_2(\mathbf{x}_j) \quad (j = 1, 2, \dots, N); \tag{13b}$$

$$(G_n)_{ij} = -kH_1^{(1)}(kr_{ij}) \left[-\frac{x_i - x_j}{r_{ij}} \left(\frac{\partial y}{\partial s} \right)_j + \frac{y_i - y_j}{r_{ij}} \left(\frac{\partial x}{\partial s} \right)_j \right] \Delta s_j \quad (i, j = 1, 2, \dots, N; i \neq j); \tag{13c}$$

$$(G_n)_{ii} = \frac{i}{\pi} \left(\frac{\partial x}{\partial s} \frac{\partial^2 y}{\partial s^2} - \frac{\partial^2 x}{\partial s^2} \frac{\partial y}{\partial s} \right)_i \Delta s_i \quad (i = 1, 2, \dots, N); \tag{13d}$$

$$(G)_{ij} = H_0^{(1)}(kr_{ij}) \Delta s_j \quad (i, j = 1, 2, \dots, N; i \neq j); \tag{13e}$$

$$(G)_{ii} = \left[1 + i \frac{2}{\pi} \left[\log \left(\frac{k\Delta s_i}{4} \right) - 0.42278 \right] \right] \Delta s_i \quad (i = 1, 2, \dots, N). \tag{13f}$$

In deriving the expression for the diagonal elements of the matrix G_n , i.e. $(G_n)_{ii}$, the asymptotic formulae of $H_1^{(1)}(kr) \sim -i(2/\pi)(1/kr)$ (for $kr \rightarrow 0$) was used. Similarly, the asymptotic formula of $H_0^{(1)}(kr) \sim 1 + i(2/\pi)(\log \frac{1}{2}kr + \gamma)$ for $kr \rightarrow 0$ (where $\gamma = 0.577215\dots$ called Euler's constant) was used for the diagonal elements of matrix G .

The vector \mathbf{P} in (13b) involves the unknown value of $\partial f_2/\partial n$ at the harbour entrance as well as the value of $\partial f_2/\partial n$ at the solid boundary (these latter values are zero). Thus, the vector \mathbf{P} can be represented as follows:

$$\mathbf{P} = \sum_{j=1}^p \delta_{ij} C_j = U_m \mathbf{C}, \quad \text{for } j = 1, 2, \dots, p, i = 1, 2, \dots, N, \tag{14}$$

where p is the total number of segments into which the harbour entrance is divided, the matrix U_m is defined as $U_m = \delta_{ij} = 0$ for $i \neq j, 1$ for $i = j$ ($i = 1, 2, \dots, N$,

and $j = 1, 2, \dots, p$), and the vector \mathbf{C} represents the p unknown values of $\partial f_2/\partial n$ at the harbour entrance.

Substituting (14) into (12) and rearranging, one obtains

$$\mathbf{X} = (\frac{1}{2}iG_n + I)^{-1} (\frac{1}{2}iGU_m) \mathbf{C} = M\mathbf{C}, \tag{15}$$

where I is the identity matrix, $(\frac{1}{2}iG_n + I)^{-1}$ represents the inverse of the matrix $(\frac{1}{2}iG_n + I)$. The matrix $M = (\frac{1}{2}iG_n + I)^{-1} (\frac{1}{2}iGU_m)$ is a $N \times p$ matrix and can be computed directly.

Equation (15) shows that the function $f_2(\mathbf{x}_i)$ on the boundary can be expressed as a function of the unknown value of $\partial f_2/\partial n$ at the entrance, i.e.

$$f_2(\mathbf{x}_i) = \sum_{j=1}^p M_{ij} C_j, \tag{16}$$

where $i = 1, 2, \dots, N$. Equation (16) can also be interpreted as the contribution to the value of f_2 on the harbour boundary from the superposition of the effect of p small harbour openings.

In order to evaluate the unknowns, C_1, C_2, \dots, C_p in (16), the function f_1 in region I at the harbour entrance must be expressed as a function of the same normal derivatives, C_1, C_2, \dots, C_p . By matching these wave functions f_1 and f_2 at the harbour entrance, i.e. equating water surface amplitudes at the entrance, the value of C_1, C_2, \dots, C_p can be determined and the complete solution to the response problem can be obtained.

(2) *Function f_1 outside the harbour (region I)*. Because the present analytical treatment is linear the function f_1 in region I can be expressed as

$$f_1 = f_i + f_r + f_3, \tag{17}$$

where f_i represents an incident wave function, f_r represents a reflected wave function considered to occur as if the harbour entrance were closed, and f_3 (termed radiated wave function) represents a correction to f_r due to the presence of the harbour. It should be noted that (17) implies that the wave amplitude in region I, $\eta_1 = A_i f_1 \exp(-i\sigma t)$, is equivalent to $\eta_1 = A_i (f_i + f_r + f_3) \exp(-i\sigma t)$.

The incident wave function, f_i , can be specified in an arbitrary fashion; for example, a periodic incident wave with the wave ray at an angle α to the x axis (the coastline in figure 2) can be represented as

$$f_i(x, y) = \exp [ik(x \cos \alpha + y \sin \alpha)].$$

The reflected wave function f_r can be represented by $f_r(x, y) = f_i(x, -y)$. For the case of a periodic incident wave with the wave ray perpendicular to the coastline ($\alpha = 90^\circ$), the function $f_i(x, y)$ can be represented by $\frac{1}{2} \exp(iky)$; the factor $\frac{1}{2}$ is chosen for convenience. (This is the case which was treated experimentally in this study and therefore the following discussion will be concerned with periodic waves normally incident to the coastline.)

The function f_1 in (17) must satisfy the Helmholtz equation in region I (equation (5)) and the following boundary conditions: (i) $\partial f_1/\partial n = 0$ on boundary \overline{AC} and $\overline{BC'}$ (as shown in figure 2). (ii) $\partial f_1/\partial n = -\partial f_2/\partial n$ on boundary \overline{AB} (harbour entrance), and (iii) $\lim_{r \rightarrow \infty} f_1 = f_i + f_r$ and the radiation condition (where $r^2 = x^2 + y^2$).

As mentioned earlier the function f_r is known once the function f_i is specified. In order to complete the evaluation of the function f_1 the main problem is to evaluate the function f_3 . The boundary condition (ii) just mentioned can be replaced by $\partial f_3/\partial n = -\partial f_2/\partial n$ at the harbour entrance, because in reference to figure 2, $\partial(f_i+f_r)/\partial n = \partial(f_i+f_r)/\partial y$ and this derivative is equal to zero on the boundary $\overline{ABC'}$. Therefore, the function f_3 in region I can be formulated as:

$$\frac{\partial^2 f_3}{\partial x^2} + \frac{\partial^2 f_3}{\partial y^2} + k^2 f_3 = 0, \tag{18}$$

with the following boundary conditions:

- (i) $\partial f_3/\partial n = 0$ on boundary \overline{AC} and $\overline{BC'}$,
- (ii) $\partial f_3/\partial n = -\partial f_2/\partial n$ on boundary \overline{AB} (harbour entrance), and
- (iii) $\lim_{r^2 \rightarrow \infty} f_3 = 0$ and the radiation condition (where $r^2 = x^2 + y^2$).

By using Weber's formula as was done in obtaining (8) the function f_3 can be expressed as

$$f_3(\mathbf{x}) = -\frac{1}{4}i \int_s \left[f_3(\mathbf{x}_0) \frac{\partial}{\partial n} (H_0^{(1)}(kr)) - H_0^{(1)}(kr) \frac{\partial}{\partial n} (f_3(\mathbf{x}_0)) \right] ds(\mathbf{x}_0), \tag{19}$$

where \mathbf{x}_0 is the source point $(x_0, 0)$ along the x axis, \mathbf{x} is the field point (x, y) in region I, and $r = [(x - x_0)^2 + y^2]^{\frac{1}{2}}$. The fundamental solution $H_0^{(1)}(kr)$ is necessary in order to satisfy the radiation condition (see Lee 1969). If \mathbf{x} approaches the x axis at the point $(x_i, 0)$ one obtains (20) which is similar to (10).

$$f_3(x_i, 0) = -\frac{1}{2}i \int_s \left[f_3(x_0, 0) \frac{\partial}{\partial n} (H_0^{(1)}(kr)) - H_0^{(1)}(kr) \frac{\partial}{\partial n} (f_3(x_0, 0)) \right] ds(x_0, 0). \tag{20}$$

The term $\partial[H_0^{(1)}(kr)]/\partial n$ inside the integral is equal to $-kH_1^{(1)}(kr) \partial r/\partial n$; however, because the points $\mathbf{x}_i(x_i, 0)$ and $\mathbf{x}_0(x_0, 0)$ are all on the x axis, $\partial r/\partial n$ equals zero. Also, the term $\partial f_3(x_0, 0)/\partial n$ is equal to zero except at the harbour entrance. Thus, (20) can be simplified to:

$$\begin{aligned} f_3(x_i, 0) &= -\frac{1}{2}i \int_{\overline{AB}} H_0^{(1)}(kr) \frac{\partial}{\partial n} [f_3(x_0, 0)] dx_0 \\ &\approx -\frac{1}{2}i \sum_{j \neq i}^p H_0^{(1)}(k|x_i - x_j|) C_j \cdot \Delta s_j - \frac{1}{2}i C_i \int_0^{\frac{1}{2}\Delta s_i} 2 \left[1 + i \frac{2}{\pi} (\log(\frac{1}{2}kr) + \gamma) \right] dr, \end{aligned} \tag{21}$$

where x_i, x_j are the mid-points of the i th and j th segments of the harbour entrance respectively, Δs_j is the length of the j th segment of the harbour entrance, the term C_j in (21) is the value of $\partial f_2/\partial n$ at the mid-point of the j th entrance segment, and p is, as before, the total number of segments into which the entrance is divided.

By substituting (21) into (17) the function f_1 at the harbour entrance can be represented as:

$$f_1(\mathbf{x}_i) = 1 + (-\frac{1}{2}i) \sum_{j=1}^p H_{ij} C_j \quad (\text{for } i = 1, 2, \dots, p). \tag{22}$$

The first term on the right-hand side of (22) represents the incident plus reflected wave if the entrance is closed and for convenience it is chosen as unity.

The second term is rewritten from (21) representing the contribution of the function f_3 , where

$$H_{ij} = H_0^{(1)}(kr_{ij}) \Delta s_j \quad \text{for } i, j = 1, 2, \dots, p; i \neq j,$$

and $H_{ii} = [1 + i(2/\pi)(\log(\frac{1}{4}k\Delta s_i) - 0.42278)] \Delta s_i \quad \text{for } i = 1, 2, \dots, p.$

(3) *Matching solution for each region at the harbour entrance.* In order to solve for the unknown value of $\partial f_2/\partial n$ at the harbour entrance, C_j , shown in (16) and (22), the condition that the water surface must be continuous at the entrance is used. This matching procedure is done in the following manner.

Take the first p equations from (16) for the value of f_2 at the harbour entrance, i.e.

$$f_2(\mathbf{x}_i) = \sum_{j=1}^p M_{ij} C_j = M_p \cdot \mathbf{C}, \tag{23}$$

in which the index $i = 1, 2, \dots, p$. (Note that the matrix M_p in (23) is a $p \times p$ matrix obtained from the first p rows of the matrix M .)

Equating (22) to (23), i.e. $f_1(\mathbf{x}_i) = f_2(\mathbf{x}_i)$, for $i = 1, 2, \dots, p$, the following matrix equation is obtained:

$$M_p \mathbf{C} = \mathbf{1} - \frac{1}{2} i H \mathbf{C}, \tag{24a}$$

$$\mathbf{C} = (M_p + \frac{1}{2} i H)^{-1} \cdot \mathbf{1}, \tag{24b}$$

where $(M_p + \frac{1}{2} i H)^{-1}$ is the inverse of the matrix $(M_p + \frac{1}{2} i H)$, and $\mathbf{1}$ is the vector with each p element equal to unity.

With the value of $\partial f_2/\partial n$ at the harbour entrance, i.e. C_j for $j = 1, 2, \dots, p$, determined from this matching procedure the value of $f_2(\mathbf{x}_i)$ at the boundary can now be calculated from (16), and the value of $f_2(\mathbf{x})$ at any position \mathbf{x} inside the harbour can be determined from the following discrete form of (8):

$$f_2(\mathbf{x}) = -\frac{1}{4} i \left\{ \sum_{j=1}^N f_2(\mathbf{x}_j) \left[-k H_1^{(1)}(kr) \frac{\partial r}{\partial n} \right] \Delta s_j - \sum_{j=1}^p H_0^{(1)}(kr) C_j \Delta s_j \right\}, \tag{25}$$

where \mathbf{x}_j is at the mid-point of j 'th boundary segment, and $r = |\mathbf{x} - \mathbf{x}_j|$.

In order to better describe the response of a harbour to incident waves a parameter called the 'amplification factor' is defined. This is the ratio of the wave amplitude at any position (x, y) inside the harbour to the sum of the incident and the reflected wave amplitude at the coastline (with the harbour entrance closed)

$$R = \frac{|\eta_2(x, y; t)|}{|A_i(f_i + f_r) \exp(-i\sigma t)|} = \frac{|A_i f_2(x, y) \exp(-i\sigma t)|}{|A_i \cdot 1 \cdot \exp(-i\sigma t)|} = |f_2(x, y)|. \tag{26}$$

Since the function $f_2(x, y)$ is a complex number the absolute value is taken when computing the wave amplitude.

With the function $f_2(x, y)$ determined, the calculation of velocity potential $\Phi(x, y, z; t)$ for the region inside the harbour is now complete (see (7)) and other quantities of interest such as the water particle velocities can be determined from this.

2.2. Circular and rectangular harbour theories

The theory developed in § 2.1 can be used for harbours of any shape. However, if the harbour is a special shape, such as circular or rectangular, the solution of the Helmholtz equation in region II can be easily obtained using the method

of separation of variables. For the open-sea (region I) the solution developed in §2.1 can be applied again. By matching the solution in both regions at the harbour entrance (for circular harbours, the arc and the chord at the entrance are assumed to be equivalent) the complete solution of the wave-induced oscillations in circular or rectangular harbours can be obtained. Since the analytic method for these special cases is quite straight-forward it will not be presented here, the interested reader is referred to Lee (1969) for detailed derivations. In §§4.1 and 4.2, theoretical solutions obtained by using these special theories for two circular harbours and a rectangular harbour will be compared with solutions given by the general theory and with experimental data.

3. Experimental apparatus

A series of experiments was conducted in the laboratory in a wave basin 1 ft. 9 in. deep, 15 ft. 5 in. wide, and 31 ft. 5 in. long. The vertical walls of the basin were constructed of $\frac{3}{4}$ in. marine plywood with the floor constructed of 1 in. marine plywood. The bottom of the wave basin was treated with a layer of polyester resin approximately $\frac{1}{4}$ in. thick and was horizontal to within at least ± 0.02 in.

The wave generator was a pendulum type 11 ft. 8 in. long, 2 ft. high located at one end of the basin and it was designed to operate either as a paddle- or piston-type wave generator; its detailed description and design consideration were given by Raichlen (1965). When operating as a paddle-type generator for short period waves the imaginary hinge point was located close to the bottom of the generating plate. Wave periods ranging from 0.34 sec to 3.8 sec and a maximum stroke of 12 in. can be obtained with this system.

The wave period was determined by measuring, with a photo-cell circuit and an electronic counter, the rotational speed of a perforated disk attached to one eccentric of the wave-generating mechanism. Wave amplitudes were measured electronically using resistance wave gauges and an oscillograph recorder. The wave gauge was calibrated before and after an experiment (approximately one hour apart). A calibration curve representing an average over the duration of an experiment was used in reducing the experimental data.

The theories developed in previous sections treat the case of a harbour connected to the open-sea which leads to the existence of the 'radiation condition', i.e. the radiated waves which emanate from the harbour entrance decay to zero at an infinite distance from the harbour. However, in the laboratory, experiments must be conducted in a wave basin of finite size; thus, the radiated waves from the harbour will be reflected from the wave paddle and the sidewalls of the basin unless effective energy dissipators are provided. Indeed it was shown by Raichlen & Ippen (1965) that the response of a rectangular harbour in a highly reflective basin is radically different from that of a similar harbour connected to the open-sea. In order to simulate the open-sea in the laboratory basin, two types of wave energy dissipators were employed in the present experiments: a wave filter placed in front of the wave generator, and wave absorbers located along the

side-walls of the wave basin. The wave filter was 11 ft. 9 in. long, 1 ft. 4 in. high and 5 ft. thick in the direction of wave propagation and was constructed of 70 sheets of galvanized iron wire screen (each sheet spaced 0.8 in. apart). The wire diameter of the screens was 0.011 in. with 18 wires per inch in one direction and 14 wires per inch in the other. The wave absorbers, placed along the side-walls of the basin were each 1 ft. 6 in. high, 1 ft. 10 in. thick, and 30 ft. long and consisted of 50 layers (spaced $\frac{3}{8}$ in. between layers) of the same galvanized iron screen as used in the wave filter. A typical wave had its amplitude reduced by about 80% as the result of passing through the wave absorber (or filter), reflecting from the wall, and passing through the wave absorber again. (In order to control corrosion of the galvanized wire screens sodium dichromate ($\text{Na}_2\text{Cr}_2\text{O}_7$) was added to the water in the basin.)

Four different harbours with constant depth were investigated experimentally: a rectangular harbour, a circular harbour with a 10° opening, a circular harbour with a 60° opening, and an example of a complicated-shaped harbour (a model of the East and West Basins of the Long Beach Harbour, California). The harbour models were designed so that each would fit into an opening at the centre of a false wall simulating a perfectly reflecting coastline which was installed 27 ft. 6 in. from and parallel to the wave paddle.

4. Presentation and discussion of results

4.1. Circular harbour with a 10° and a 60° opening

In this section the theoretical results obtained by using the theories developed in §§ 2.1 and 2.2 are compared to the experimental results for harbours with a 10° and a 60° opening. The results will be presented as: (i) the variation of the amplification factor at a fixed position inside the harbour as a function of incident wave-number, (ii) the variation of the wave amplitude inside the harbour for some resonant modes.

(1) *Response of harbour to incident waves.* The response of a harbour is defined, for this study, as the variation of the amplification factor, R , with the wave-number parameter ka (wherein R is defined in (26), k is the wave-number and a is a characteristic planform dimension of the harbour, in this case a is the radius of the circular harbour). Response curves at an arbitrarily chosen point ($r = 0.7$ ft., $\theta = 45^\circ$) inside a circular harbour with a 10° opening are presented in figure 3. In the figure the solid line represents the theoretical curve computed from the theory for an arbitrary shape harbour (§ 2.1); the theory for the circular harbour (§ 2.2) is shown with dashed lines. The experiments were conducted using a circular harbour of 1.5 ft. diameter with the depth of water constant and equal to 1 ft. in both the harbour and the 'open-sea'. The experimental amplification factor was obtained by dividing the wave amplitude at the point investigated inside the harbour ($r = 0.7$ ft., $\theta = 45^\circ$) by the average wave amplitude of the standing wave system at the harbour entrance (when the entrance is closed).

For a circular harbour with a 10° opening the arc and the chord at the harbour entrance are nearly the same; therefore, the circular harbour theory (§ 2.2) should give accurate results when applied to this harbour. In using the circular harbour

theory the averages (across the entrance) of the wave functions, f_2 and f_1 , and their normal derivatives $\partial f_2/\partial n$ and $\partial f_1/\partial n$, were matched at the harbour entrance. In using the arbitrary-shape harbour theory, the boundary of the circular harbour including the entrance was divided into 36 segments with each segment having a 10° central angle. Since the harbour entrance was represented by one of these segments only one unknown complex value of $\partial f_2/\partial n$ needs to be evaluated by the matching procedure described in §2.1. Calculations were also made with the arbitrary-shape harbour theory when the harbour entrance was divided into

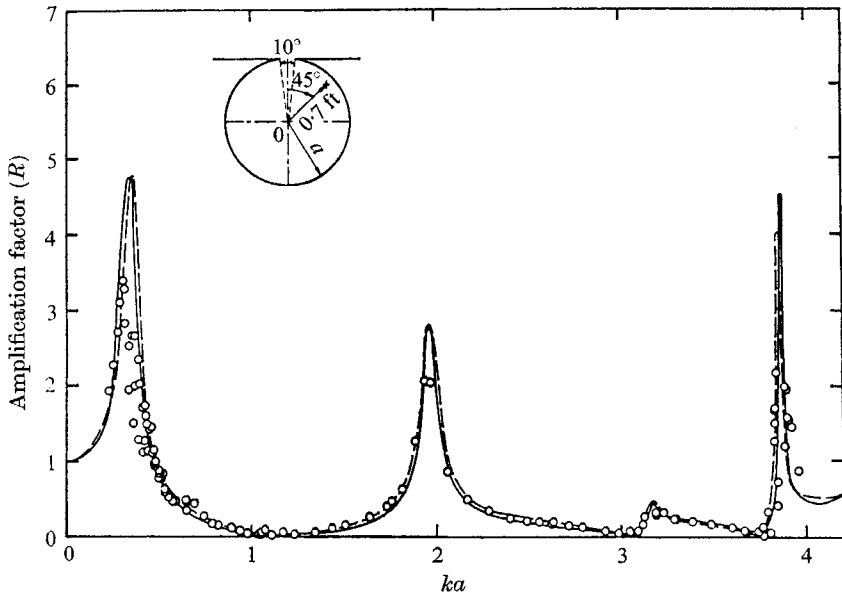


FIGURE 3. Response curve at $r = 0.7$ ft., $\theta = 45^\circ$ of the circular harbour with a 10° opening. —, arbitrary-shape harbour theory; ---, circular harbour theory; O, experiment ($a = 0.75$ ft.).

five segments, i.e. each entrance segment includes 2° central angle. These results (not presented here) agree within 2% of those presented in figure 3 which were obtained by considering one entrance segment. No calculations were made with the circular harbour theory using more than one entrance segment.

In figure 3 the experimental data and the theoretical results agree well. Since the energy dissipation due to viscous effects has not been considered in the theories, the theoretical values of the amplification factor near resonance are, as expected, larger than the experimental values. There are four distinct modes of resonant oscillations in the range of ka that are presented in figure 3; the value of ka for these four are 0.35, 1.988, 3.18, and 3.87. (It is noted that except for the first mode ($ka = 0.35$) which does not exist in the completely-closed basin, each mode corresponds to a mode of free oscillation in closed circular basins which occur at $ka = 1.84, 3.05, \text{ and } 3.83$.)

A similar response curve for the circular harbour with a 60° opening (for position corresponding to those shown in figure 3) is presented in figure 4. As

before, theoretical curves obtained from each of the theories are shown. In using the theory for an arbitrary-shape harbour, the boundary of the harbour (including the entrance) was divided into 36 segments, and for this case the entrance was represented by six of these boundary segments. Therefore, six complex constants of $\partial f_2/\partial n$ at the harbour entrance, i.e. C_j for $j = 1, 2, \dots, 6$, were determined by the matching procedure. When applying the circular harbour theory, the average value of $\partial f_2/\partial n$ across the entrance was determined by the matching

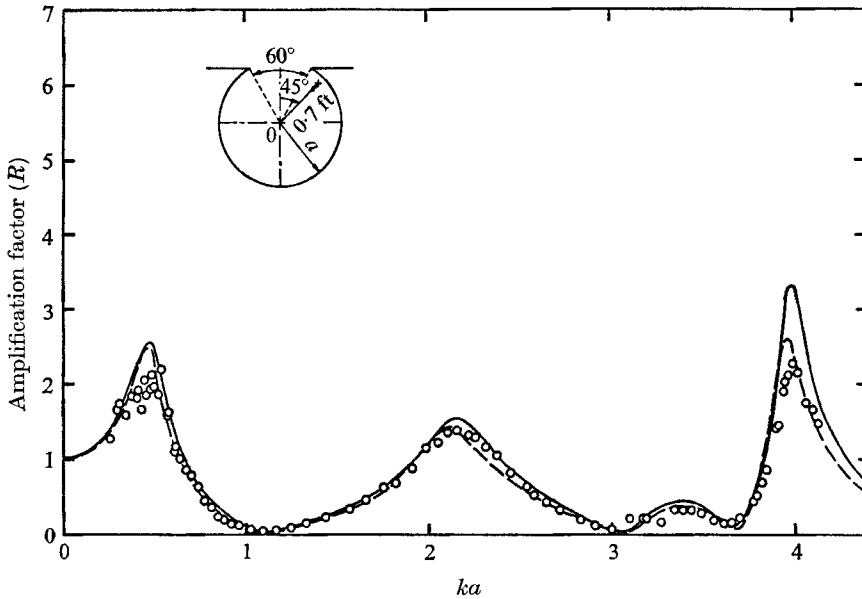


FIGURE 4. Response curve at $r = 0.7$ ft., $\theta = 45^\circ$ of the circular harbour with a 60° opening. —, arbitrary-shape harbour theory; ---, circular harbour theory; O, experiment ($a = 0.75$ ft.).

procedure as for the case of a 10° opening. The theoretical results presented in figure 4 also shows good agreement with the experimental data. The value of ka for the four modes of resonant oscillation (corresponding to those for the case of a 10° opening) are 0.46, 2.15, 3.38, and 3.96.

By comparing figure 3 with figure 4 the effect of the size of the harbour opening on the amplification of waves inside the harbour can be observed. It is obvious from these figures that the maxima which appeared in figure 3 for the harbour with a 10° opening are replaced by peaks of smaller amplification factors and larger band widths for the harbour with a 60° opening. This effect was called the 'harbour paradox' by Miles & Munk (1961). In addition, it is seen that for the 60° opening, the values of ka of the modes of resonant oscillation are larger than the values of ka for the corresponding modes for the harbour with a 10° opening indicating that the value of ka at resonance approaches the value for a closed basin as the entrance width decreases. It is also seen that the theoretical results agree with the experimental data better for the harbour with the larger opening.

This may imply that the effect of viscous dissipation, which has not been considered in the theories, is most important for the harbour with a smaller opening.

(2) *Variation of wave amplitude inside the harbour for some resonant modes.* The results which deal with the response curves have demonstrated that the two theories agree well with the experimental data. Both theories are tested further by comparing the theoretical results with the experimental data for the wave-amplitude distribution inside the harbour for certain values of ka .

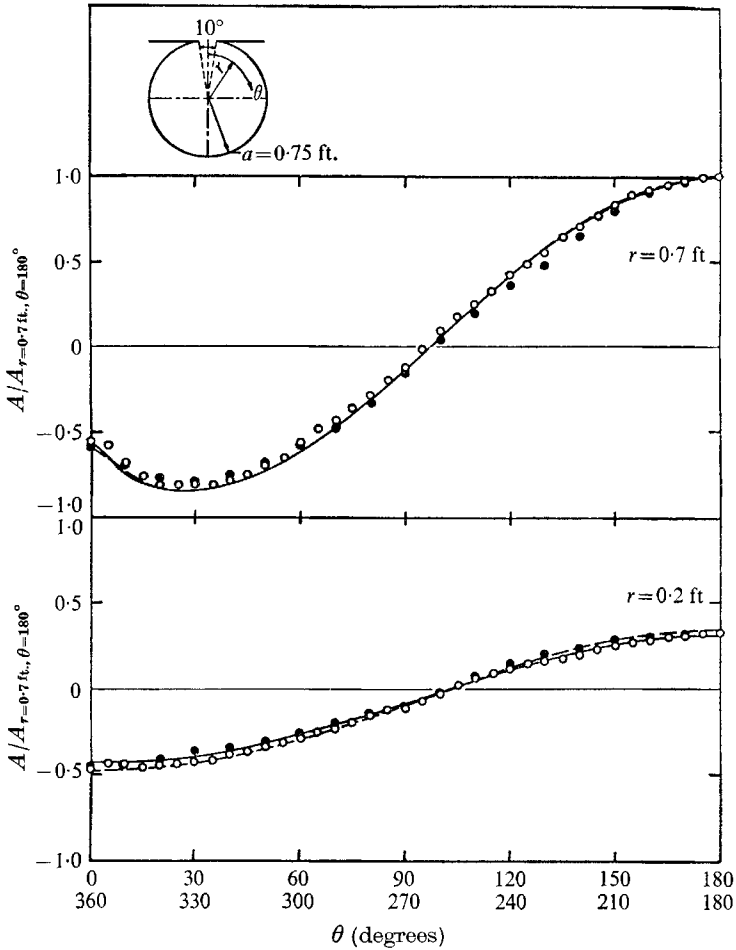


FIGURE 5. Wave-amplitude distribution inside the circular harbour with a 10° opening for $ka = 1.988$. —, arbitrary-shape harbour theory; ---, circular harbour theory; \circ , experiment ($0 \leq \theta \leq 180^\circ$); \bullet , experiment ($180^\circ < \theta \leq 360^\circ$).

Figure 5 shows the wave-amplitude distribution along two circular paths with $r = 0.7$ ft. ($r/a = 0.935$) and $r = 0.2$ ft. ($r/a = 0.267$) for $ka = 1.988$ for the harbour with a 10° opening. The ordinate in figure 5 is the relative wave amplitude normalized with respect to the wave amplitude at the position of $r = 0.7$ ft, $\theta = 180^\circ$ which is the maximum amplitude among the points measured. This value of ka corresponds to the second maximum in the response curve shown in

figure 3. It is seen that the two theories agree well with the experiments at the locations where measurements were made. Figure 5 shows, for $r = 0.7$ ft. a region of negative water surface displacements (negative wave amplitudes) for $0^\circ \leq \theta < 97^\circ$ with positive displacements for $97^\circ < \theta \leq 180^\circ$. Similarly, for

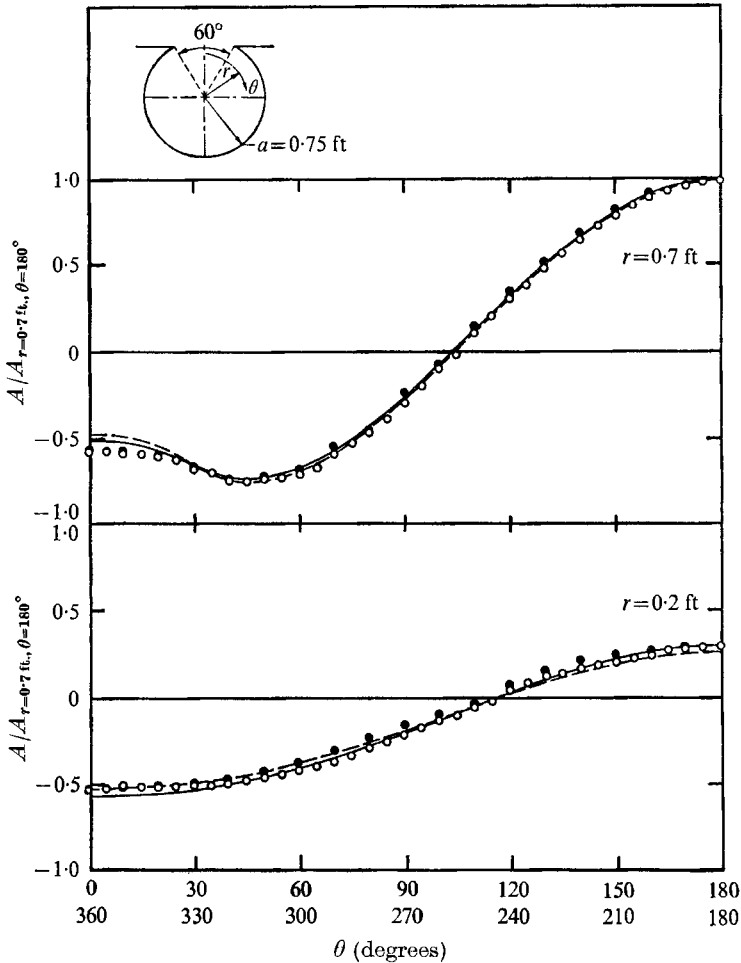


FIGURE 6. Wave-amplitude distribution inside the circular harbour with a 60° opening for $ka = 2.153$. —, arbitrary-shape harbour theory; ---, circular harbour theory; \circ , experiment ($0 \leq \theta \leq 180^\circ$); \bullet , experiment ($180^\circ < \theta \leq 360^\circ$).

$r = 0.2$ ft. two regions are seen with opposite phase, i.e. $0^\circ \leq \theta < 103^\circ$ with negative displacements and $103^\circ < \theta \leq 180^\circ$ with positive displacements.

Figure 6 shows the wave-amplitude distribution along radii $r = 0.7$ ft. and $r = 0.2$ ft. at $ka = 2.153$ for the harbour with a 60° opening. This value of ka is the same as for the second maximum in the response curve presented in figure 4. It can be seen that the general shape of the water surface (wave-amplitude distribution) is similar to the one shown in figure 5 for the case of a 10° opening. For this case the intersections of the nodal line with the chosen circular paths occur

at larger values of θ : 105° for $r = 0.7$ ft. and 116° for $r = 0.2$ ft. This indicates that the nodal line for this mode of oscillation is located closer to the backwall region than for the case of a 10° opening.

The response curves and the amplitude distribution curve presented have demonstrated the agreement between the theories and experiments. A questionable element in the circular harbour theory (§ 2.2) is in the small entrance approximation where the arc and the chord at the entrance are considered to be equivalent. The results have shown that this approximation still applies well for the case of a 60° opening; thus, it appears that for this type of solution the small entrance approximation can be applied at least up to a 60° opening. It is fair to say that the good agreement between the two theories, as well as between the experimental data and these theories, confirms the applicability of the arbitrary-shape harbour theory to the first extreme case: a curved boundary with a tangent continuously changing direction. The application of the arbitrary-shape harbour theory for the second extreme case, a harbour composed of straight-lined boundaries will be presented and discussed in the next section.

4.2. Rectangular harbour

The response of a fully-open rectangular harbour ($2\frac{3}{8}$ in. wide, $12\frac{1}{4}$ in. long) to periodic incident waves is presented in figure 7. The abscissa is the parameter kl (where l is the length of the harbour); the ordinate is the amplification factor, R , defined as the wave amplitude at the centre of the backwall of the harbour (point A) divided by the average standing wave amplitude at the harbour entrance when the entrance is closed. Three theoretical curves are shown (the arbitrary-shape harbour theory in solid lines (§ 2.1), the rectangular harbour theory in long dashed lines (§ 2.2), the theory of Ippen & Goda (1963) in short-dashed lines). The experimental data obtained from the present study (with the water depth equal to 0.844 ft.) are denoted by open circles while the experimental data of Ippen & Goda (1963) are shown as solid circles.

In using the arbitrary-shape harbour theory (§ 2.1) the boundary of the harbour is divided into 47 segments ($N = 47$) of unequal length including three segments at the harbour entrance. For the rectangular harbour theory only the averaged value of $\partial f_2 / \partial n$ across the harbour entrance is matched. Thus, the only difference between the theory of Ippen & Goda (1963) and the present rectangular harbour theory lies on the evaluation of the function f_3 . The former used the Fourier transformation method to evaluate the function f_3 while the present theory applies Weber's solution of the two-dimensional Helmholtz equation. From figure 7 it is seen that any differences between these two appears to be quite small.

From figure 7 it is seen that the three theoretical curves all agree fairly well with the experimental results and that the present experimental data agree better with the theoretical curves than do the experimental data of Ippen & Goda (1963), especially in the vicinity of resonance. This is probably because the wave basin for present experiments is both wider and longer than the one used by Ippen & Goda, hence the incident wave is more nearly two-dimensional; also the present energy dissipators are more efficient than those used by Ippen &

Goda and therefore the 'open-sea' condition is simulated more satisfactorily. This is supported by the fact that the data of Ippen & Goda show fluctuations in the response curve especially in the region $1.10 < kl < 1.70$ indicating that the 'open-sea' condition is not properly simulated in this frequency range where the wavelength is large and the wave energy dissipators are correspondingly less efficient than for shorter wavelengths. Such fluctuations do not appear in the present experimental data.

The agreement between the theories and the experimental data as shown in figure 7 has demonstrated that the arbitrary-shape harbour theory can also be applied successfully to a harbour with straight sides and sharp interior corners.

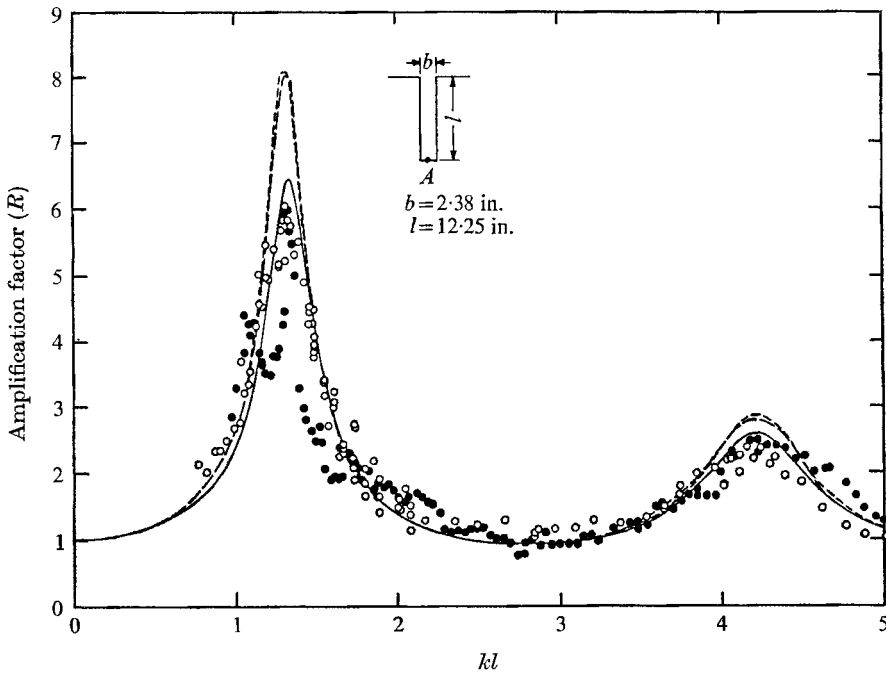


FIGURE 7. Response curve at the centre of the backwall (point *A*) of a fully-open rectangular harbour. —, arbitrary-shape harbour theory; - - -, rectangular harbour theory; - · - ·, theory of Ippen & Goda (1963); O, present experiment; ●, experiment by Ippen & Goda (1963).

4.3. An example of a harbour with complicated shape

In order to test the arbitrary-shape harbour theory further, a harbour of complicated shape was studied both theoretically and experimentally. In planform this harbour model is slightly modified from the existing harbour of the East and West Basins of the Long Beach Harbour (with a horizontal scale 1 to 4700). The water depth of the prototype harbour is fairly uniform with an average depth of 40 ft.; the water depth of the harbour model is 1 ft. (A sketch of the harbour shape is included in figure 8.)

A response curve at an arbitrarily-chosen location inside the harbour (designated as point *A*) is presented in figure 8. If the right-hand corner of the harbour

opening is taken as the origin of co-ordinates (x axis lies on the coastline) then in model dimensions the co-ordinates of point A can be specified as: A (1.42 ft., -0.96 ft.), where the first number inside the bracket is the x co-ordinate and the second number is the y co-ordinate. As before, the abscissa in the response curve is the parameter ka (where again k is the wave-number and a is the characteristic length equal to 1.44 ft. for this particular harbour model); the ordinate is the amplification factor R which is defined as the wave amplitude at point A divided by the average standing wave amplitude at the harbour entrance when the harbour is closed.

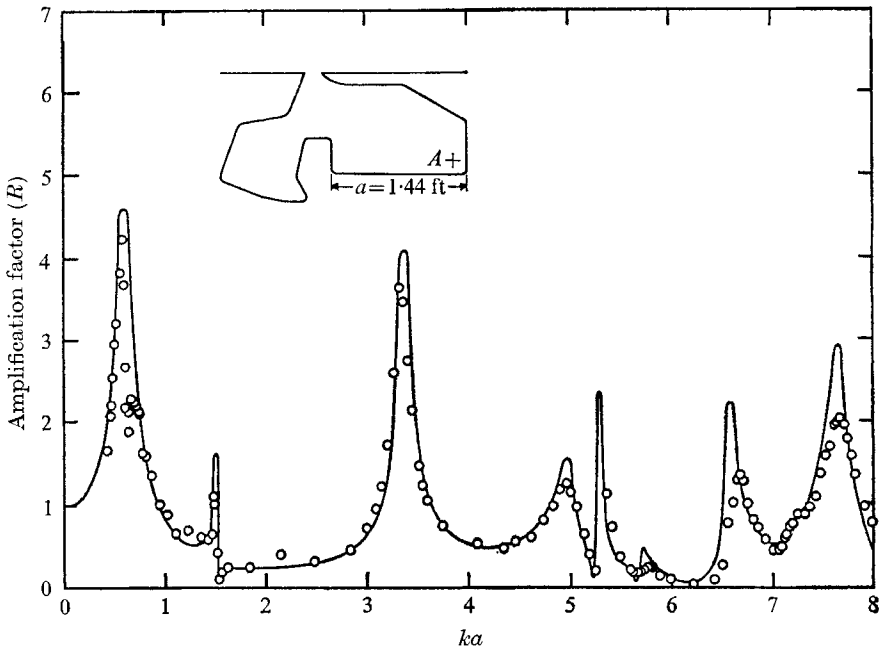


FIGURE 8. Response curve at point A of the Long Beach Harbour model.
—, arbitrary-shape harbour theory; O, experiment.

In applying the arbitrary-shape harbour theory the boundary of the harbour is divided into 75 unequal straight-line segments including two segments for the entrance. It is seen that the theoretical results agree well with the experimental data and show that the response of this harbour to periodic waves is much more complicated than the response curves for either a circular or a rectangular harbour. From the response curve it is also seen that while the theory has predicted the frequency of every resonant mode of oscillation correctly, the theoretical amplification factor at resonance is slightly larger than the measured value especially for the resonant modes at larger values of ka . It can be imagined that in using the same number of segments for the boundary of the harbour at all wave periods the theoretical results for a smaller value of ka are more accurate than the results which correspond to large ka . (Since for the former case the ratio of the length of the boundary segments to the wavelength is smaller than

that of the latter case.) This may contribute to the fact that a better agreement, between the theory and the experiments, at smaller values of ka is observed. These results have demonstrated again the applicability of the arbitrary-shape harbour theory to a harbour of complicated planform.

It was mentioned in §2.1 that in using the theory for an arbitrary-shape harbour, the boundary of the harbour must be divided into a sufficiently large number of segments. 'Sufficient' implies that the results obtained using this approximate theory must agree with the exact solution within an allowable limit. For practical purposes, the following considerations must be given to the relative size of each segment: when the boundary is divided and replaced by straight-line segments these must be a good approximation to the actual boundary, and the length of each straight-line segment, Δs , must be small compared with the wavelength, L . This second criterion can be represented best by the parameter $k\Delta s$ (where k is the wave-number). Among the four harbour models used in this study the largest value of $k\Delta s$ was 0.69. Judging by the good agreement realized between the present theory and the experimental results for the three different boundary configurations, it is concluded that the boundary of the harbour models were divided into segments which were sufficiently small; this criterion corresponds to the ratio $\Delta s/L \approx \frac{1}{9}$. Therefore, a conservative statement of the criterion for segment length can be stated as: the harbour perimeter should be divided into a number of ' N ' straight-line segments such that the ratio of the length of the largest segment to the smallest wavelength to be considered is less than about one-tenth.

The author wishes to thank his thesis advisor, Professor Fredric Raichlen, for suggesting this problem and offering guidance and encouragement throughout the course of this study. Thanks are also due to other members of the thesis committee and the staff of the W. M. Keck Laboratory of Hydraulics and Water Resources, who helped with various phases of this study. This work was supported by the U.S. Army Corps of Engineers under Contract no. DA-22-079-CIVENG-64-11.

REFERENCES

- BAKER, B. B. & COPSON, E. T. 1950 *The Mathematical Theory of Huygen's Principle*. Oxford University Press.
- BANAUGH, R. P. & GOLDSMITH, W. 1963 Diffraction of steady acoustic waves by surfaces of arbitrary shape. *J. Acoust. Soc. Am.* **35**, 1590-1601.
- HWANG, L. S. & TUCK, E. O. 1970 On the oscillations of harbours of arbitrary shape. *J. Fluid Mech.* **42**, 447-464.
- IPPEN, A. T. & GODA, Y. 1963 Wave-induced oscillations in harbours: the solution for a rectangular harbour connected to the open-sea. *Hydrodynamics Lab., M.I.T. T.R.* no. 59.
- KRAVTCHEIKO, J. & McNOWEN, J. S. 1955 Seiche in rectangular ports. *Quart. Appl. Math.* **13**, 19-26.
- LEE, J.-J. 1969 Wave-induced oscillations in harbors of arbitrary shape, Ph.D. thesis, California Institute of Technology. (Also *W. M. Keck Lab. of Hyd. and Water Resources, Cal. Inst. Tech. Rep.* KH-R-20.)
- LEENDERTSE, J. J. 1967 Aspects of computational model for long-period water wave propagation. *The Rand Corporation Memo.* RM-5294-PR.

- McNOWN, J. S. 1952 Waves and seiche in idealized ports. *Gravity Waves Symposium, National Bureau of Standards, Cir. 521*, pp. 153-164.
- MILES, J. & MUNK, W. 1961 Harbour paradox. *Proc. Am. Soc. Civ. Engrs, J. Waterways Harbor Div.* **87**, 111-130.
- RAICHLEN, F. 1965 Wave-induced oscillations of small moored vessels. *W. M. Keck Lab. of Hyd. and Water Resources, Cal. Inst. Tech. Rep.* KH-R-10.
- RAICHLEN, F. & IPPEN, A. T. 1965 Wave-induced oscillations in harbours. *Proc. Am. Soc. Civ. Engrs, J. Hydr. Div.* **91**, 1-26.
- WILSON, B. W., HENDRICKSON, J. A. & KILMER, R. C. 1965 Feasibility study for a surge motion model of Monterey Harbour. *Science Engineering Associates, San Marino, California Rep.* 2-136.